Available online at www.sciencedirect.com

Metabolism

www.metabolismjournal.com

Role of PARL-PINK1-Parkin pathway in adipocyte differentiation

Ming-Yuh Shiau[a], *Pin-Shen Lee*[b], *Ying-Jyun Huang*[b], *Ching-Ping Yang*[b], *Chiao-Wan Hsiao*[b], *Kai-Yun Chang*[b], *Huan-Wen Chen*[b], *Yih-Hsin Chang*[b,*]

[a] *Department of Nursing, College of Medicine & Nursing, Hungkuang University, Taichung 433, Taiwan*
[b] *Department of Biotechnology and Laboratory Science in Medicine, National Yang-Ming University, Taipei 112, Taiwan*

ARTICLE INFO

Article history:
Received 15 November 2016
Accepted 23 March 2017

Keywords:
Adipogenesis
Parkin
Peroxisome proliferator-activated receptor-γ (PPARγ)
Presenilin associated rhomboid-like protein (PARL)
PTEN-induced kinase 1 (PINK1)

ABSTRACT

Objective. Adipogenesis determines the number of adipocytes which is increased when individuals become obese. Mitochondria undergo remarkable morphological and functional changes during adipogenesis. PTEN-induced kinase 1 (PINK1) is pivotal to maintain mitochondrial homeostasis in neural cells. The present study aimed at investigating effects of PINK1 on adipogenesis and energy metabolism.

Methods. Expression of presenilin associated rhomboid-like protein (PARL), PINK1 and Parkin, as well as the interaction among these proteins was temporally examined during adipogenesis. In addition, the alterations of mitochondrial mass and the energy metabolism were also analyzed.

Results. Adipogenic process can be dissected into 3 stages according to the participation of PARL-PINK1-Parkin system. (1) When pre-adipocytes are switched to differentiation, f-PINK1 is subjected to PARL cleavage to generate s-PINK1 at the early stage of differentiation (0–4 day). Mitochondrial mass is increased for generating ambient energy to meet the demands for cellular remodeling. (2) At the second stage (5–6 day), s-PINK1 persistently accumulates in mitochondria and translocates into cytoplasm to mediate Parkin degradation. Mitochondria are fragmented to reduce their mass. (3) At the late stage (7–8 day), only residual autophagy activity is remained when excess mitochondria have been eliminated. This mitochondria clearance maintains energy consumption of mature adipocytes at the minimal levels for storing energy. PARL silencing aborts adipogenesis by inhibiting PPARγ expression and the finely-orchestrated events.

Conclusions. Our findings reveal the sequential adipogenic events directed by PARL-PINK1-Parkin system, add more evidence supporting the convergence of pathogenesis leading to neurodegenerative and metabolic diseases, and provide substantial information for developing novel therapeutic strategies by manipulating adipogenesis.

Abbreviations: C/EBPα/β, CCAAT-enhancer-binding protein-α/−β; DRP1, dynamin-related protein-1; FABP4, adipocyte fatty acid binding protein-4; GSK-3β, glycogen synthase kinase-3β; IL-4, Interleukin-4; MCE, mitotic clonal expansion; Mdivi-1, mitochondria division inhibitor 1; MFN1, mitofusin-1; PARL, presenilin associated, rhomboid-like; PI3K, phospho-inositide 3-kinase; PINK1, PTEN-induced kinase 1; PPARγ, peroxisome proliferator-activated receptor gamma; PTEN, tumor suppressor phosphate and tensin homologue deleted on chromosome 10; T2DM, type 2 diabetes mellitus.

* *Corresponding author at:* Department of Biotechnology and Laboratory Science in Medicine, National Yang-Ming University, Taipei 112, Taiwan. Tel.: +886 2 28267955; fax: +886 2 28219240.
E-mail address: cyh@ym.edu.tw (Y.-H. Chang).

http://dx.doi.org/10.1016/j.metabol.2017.03.010
0026-0495/

1. Introduction

Obesity is closely associated with metabolic abnormalities and the incidence of type 2 diabetes mellitus (T2DM), hyperlipidemia, and cardiovascular diseases [1]. Obesity is characterized by an increased mass of white adipose tissue (WAT). When individuals are gaining weights, their WAT mass gradually expands by increasing adipocytes number and/or size [2]. The increase of adipocytes number is mainly due to adipocyte differentiation (adipogenesis), the generation of new adipocytes from pre-adipocytes. Pre-adipocytes undergo dramatic morphological and physiological changes during adipogenesis to be equipped with the machinery and function of mature adipocytes [3]. Therefore, adipogenesis determines the number of adipocytes, and thus, the size of body adipose reservoir. Mitochondria also undergo remarkable morphological and functional changes during adipogenesis to assure the role of mature adipocytes as the major body energy reservoir [4]. Most of the mature adipocytes contain a single large lipid droplet with very limited number of mitochondria [5].

Mitochondria maintain their functional homeostasis by dynamic fusion and fission in responding to the environments [6,7]. Mitochondrial dysfunction has long been implicated in the pathogenesis of Parkinson's disease (PD). Mutations in genes encoding PTEN-induced kinase 1 (PINK1) and Parkin lead to hereditary early-onset PD, suggesting that mitochondrial integrity is a crucial factor for PD [8–10]. PINK1 is rapidly and constitutively degraded under steady-state conditions in a mitochondrial membrane potential–dependent manner. Dysfunctional mitochondria stabilize PINK1 that recruits Parkin to mitochondrial surface for initiating degradation of damaged mitochondria. Therefore, PINK1 cooperates with Parkin to selectively eliminate dysfunctional/damaged mitochondria for maintaining mitochondrial homeostasis [11].

In addition to PD, several evidences suggest that PINK1 participates in energy metabolism. Reduced number and impaired function of mitochondria are identified in T2DM subjects, their family and in elderly [12], suggesting that mitochondrial dysfunction is a contributing factor to pre-diabetic state and diabetes. Besides, PINK1 is correlated with blood sugar and free fatty acids and PINK1 silencing impairs glucose uptake [13,14]. PINK1 and Parkin modulate PI3K pathway which is important in insulin signaling [15,16]. Moreover, not only T2DM is reported as a risk factor of PD, but PD patients with diabetes have increased PD severity [17–20]. Risk for diabetic individuals to develop PD is 1.85 times of the others without [21]. These findings raise the hypothesis that diabetes-associated metabolic stress contributes to PD development, and vice versa. However, the underlying reasons for addressing the dysregulated mitochondria in T2DM pathogenesis and the linkage between PD and T2DM leave to be explored.

In this context, we hypothesized that PINK1 plays an important role in energy metabolism, and its dysregulation leads to metabolic abnormalities such as obesity and T2DM. Adipogenesis offers an ideal model to explore the hypothesis because adipogenesis, at least in part, determines the body adipose reservoir which then modulates whole-body metabolism through endocrine functions. Therefore, the present study aimed at elucidating the effects of PINK1 on adipogenesis and energy metabolism.

2. Materials and Methods

2.1. Materials

Reagents were obtained from the following source: Antibodies against C/EBPα, PPARγ, FABP4, Akt, phospho-Ser^{473} Akt, GSK-3β, phospho-Ser^{9} GSK-3β, ubiquitin, and β-actin form Cell Signaling Technology (Danvers, MA); anti-Drp1 from Novus Biologicals (Littleton CO); antibodies against PARL, LC3B and Atg14 from GenTex (Irvine, CA); antibodies against PINK1, VDAC and Parkin from Abcam (San Francisco, CA); mouse recombinant IL-4 from Millipore (Temecula, CA); Mdivi-1 from Enzo Life Sciences; ECL reagent from Calbiochem (Merck Millipore, Billerica, MA); 3-isobutyl-methylxanthine (IBMX), dexamethasone (Dex), and insulin from Sigma (St. Louis, MO); protein A/G beads, Trizol Reagent and Applied Biosystems SYBR Green Realtime PCR Master Mix from Life Technology (Carlsbad, CA); PARL small hairpin RNA (shRNA, TRCN0000351849: 5′-GCTGTCAACG TTCAGTCATT-3′) and pLKO.1-hairpin vector from the RNAi Consortium, Academia Sinica.

2.2. Cell Culture, Adipogenesis of 3T3-L1 Cells and Oil Red O Staining

3T3-L1 preadipocytes were maintained in DMEM containing 10% calf serum (Hyclone Laboratories, South Logan, Utah) as previously described [22]. After reaching confluence for 2-days, 3T3-L1 cells (designated day 0) were induced to differentiate by addition of a standard cocktail (MDI) composed of 0.5 mM IBMX, 1 μM Dex, and 10 μg/ml insulin in 10% FBS for 2 days. The cells were then cultured in DMEM supplemented with 10% FBS and 5 μg/ml insulin. The medium was replaced by fresh medium every two days. For IL-4 and Mdivi-1 experiments, cells were allowed to differentiate under the exposure of either 10 ng/ml IL-4 or 50 uM Mdivi-1. Oil-Red O staining was performed as described. For quantification, the dye was eluted by adding 100% isopropanol and the extracts were determined by measuring the absorbance at 490 nm.

2.3. Western Blot Analysis and Immunoprecipitation Assay

Cell lysates were prepared in RIPA buffer containing protease inhibitors as described previously [22,23]. Cell extracts were subjected to SDS-PAGE, transferred to PVDF membrane and blotted with specific primary antibodies. For detection, membranes were incubated with secondary antibodies (Merck Millipore, Billerica, MA) for 1 h, and results were visualized with ECL regent and quantified by Labscan software. For immunoprecipitation assay, 500 μg cell lysates were incubated with 1 μg specific primary overnight at 4 °C and captured by protein A/G agarose for 2 h. After washing with RIPA buffer, immunoprecipitates were eluted in sample buffer, denatured, and subjected to Western blotting as described.

2.4. RT- PCR

Total RNA was isolated by TRIzol reagent according to the manufacturer's instructions. About 2 μg of total RNA was reversed transcribed with Improm-II Reverse Transcription Kit (Promega, Madison, WI);total cellular RNA was extracted using TRIzol reagents. Briefly, cDNA was synthesized using total RNA (5 μg), oligo dT primer (200 *p*mol), and 5× MMLV RT. The synthesized cDNA was amplified in SuperRed mix (TOOLS Life Science Reagent) using target sequence-specific PCR primers. All RT-PCR reactions were carried out with initial 95 °C denaturation for 5 min and the following thermocycles: 95 °C denaturation for 1 min, annealing for 1 min and 72 °C extension for 1 min. PCR products were separated by electrophoresis and visualized using an ultraviolet transilluminator. Quantitative results were presented as the mean of three independent experiments. The following primers were used for detection of the gene expression: PINK1 (5′-GATGCA CTGCCTATGAGCACTT-3′, 5′-AGAGGTCCACAGAGCTGATTCC -3′), PARL (5′- CCTATAAGAACACTCGTGAAGCC-3′, 5′-CCAGT CAGCTTTTATGCCATC-3′), and GADPH (5′-AACCACAGTCCA TGCCATCAC-3′, 5′- TCCACCACCCTGTTGCTGTA-3′).

2.5. Cell Fractionation and Mitochondrial Isolation

Cells were harvested after 5 min treatment with trypsine-EDTA (0.05% trypsin and 0.02% EDTA). Cells were harvested and homogenized with mitochondria isolation buffer (225 mM mannitol, 75 mM sucrose and 2 mM K_2HPO_4, pH 7.2; BioChain Institute) by Dounce homogenizer. Homogenates were subjected to sequential differential centrifugation at 600 *g* for 10 min, and by 12,000 *g* for 15 min at 4 °C to collect the cytosol supernatant and the intact mitochondria in the sediment. The mitochondrial pellet was resuspended in lysis buffer (with 0.25% SDS, protease inhibitors, and PMSF) to harvest mitochondrial proteins. Efficiency of cell fractionation was analyzed by immunoblotting with VDAC1 and actin.

2.6. Immunofluorescence

Cells were plated on glass coverslips in tissue culture plates and allowed to grow for 24 h. Mitochondria were first stained by mitotracker red CMXRos (Invitrogen) for 3 min at 37 °C. Then the cells were fixed with 3.7% formaldehyde for 15 min and permeabilized with 0.2% triton X-100 for 15 min at room temperature. The cells were then blocked with 5% BSA for 60 min at room temperature, followed by incubation with the specific primary antibody overnight at 4 °C, then goat anti-rabbit IgG conjugated DyLight™594(Jackson ImmunoResearch Laboratories, PA) was and incubated for 1 h at room temperature. Cells were then mounted with GEL/MOUNT containing DAPI (Molecular Probes, Eugene). The images were taken by ZEISS LSM 700 confocal fluorescence microscope system using 63X objective len.

2.7. PARL Knockdown

The PARL was knocked down in 2-day postconfluent cells by lentiviral transduction of PARL- or control- shRNA constructs in pLKO.1-hairpin vector with 8 μg/mL polybrene reagent for 24 h. The medium was then replaced with DMEM supplemented with 10% calf serum, and the cells were incubated for another 24 h and induced into differentiation in the presence of puromycin. PARL mRNA and protein were analyzed as described to evaluate the efficiency of PARL knockdown.

2.8. Mitochondrial Membrane Potential

Mitochondrial membrane potential was analyzed using the cationic fluorescent dye JC-1 (5 μM; Bio Vision, Milpitas, CA). Cells were stained with fluorescence JC-1 dye at indicated time and observed by Zeiss LSM700 confocal microscopy. The monomer JC-1 showed green fluorescence (low membrane potential), while the aggregates showed red fluorescence (normal membrane potential).

2.9. Animal Experiments

Four-week-old male C57BL/6 mice were randomly divided to 3 groups: (1) WT mice were fed with standard Chow diet for 13 weeks; (2) HFD (high-fat diet) mice were fed with HFD for 13 weeks to induce insulin resistance; (3) HFD + STZ mice were fed with HFD for 13 weeks and received streptozotocin (STZ) injection (50 mg/kg; Sigma-Aldrich, St Louis, MO) for 3 times during the 9th week to induce diabetic onset. The *ob/ob* and *db/db* mice were fed with standard Chow diet for 14 weeks. Protein extracts from the harvested primary epididymal fat tissues were obtained by homogenizing the tissues using T-PER tissue protein extraction reagent (Pierce, Rockford, IL) supplied with phosphatase and protease inhibitors (Roche, Indianapolis, IN), then subjected to western analysis. Animal protocols were reviewed and approved by the Institutional Animal Care and Use Committee, National Yang-Ming University, with all the methods carried out in accordance with the approved guidelines.

2.10. Quantification of Glucose Uptake and Intracellular ATP Contents

Glucose uptake assay was performed after cells were incubated with glucose-free DMEM for 8 h. Cells were fed with 250 μmol/L 2-[N-(7-nitrobenz-2-oxa-1,3-diazol-4-yl)amino]-2-deoxy-D-glucose (2-NBDG; Cayman Chemical, Ann Arbor, Michigan) in the presence (INS) or absence (Mock) of insulin pre-treatment (100 nM for 30 min). Cellular 2-NBDG uptake was terminated after 10 min by adding ice-cold DMEM containing 10 mM glucose. Cells were washed with ice-cold PBS and lysed, and intracellular fluorescence intensity was measured (485/540 nm, Infinite 200). Intracellular ATP content was analyzed by Single Addition Luminescence ATP Detection Assay System (PerkinElmer ®, Sigma) according to the manufacturer's instructions. In brief, cells were lysed by 100 μL 1X lysis buffer containing luciferase and D-luciferin, then ATP content was measured by Infinite® 200 PRO (Tecan).

2.11. Statistical Analysis

Each experiment was carried out at least three times. Results were presented as mean ± S.E.M. and the significant difference between groups was analyzed by two-tailed unpaired Student

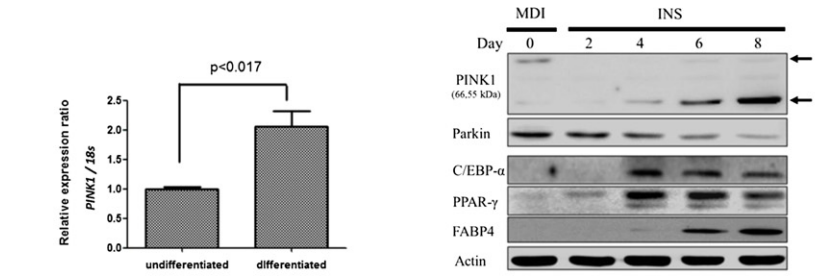
p<0.017
Relative expression ratio
PINK1 / 18s
undifferentiated
differentiated
MDI
INS
Day 0 2 4 6 8
PINK1
(66,55 kDa)
Parkin
C/EBP-α
PPAR-γ
FABP4
Actin

(A) (B)

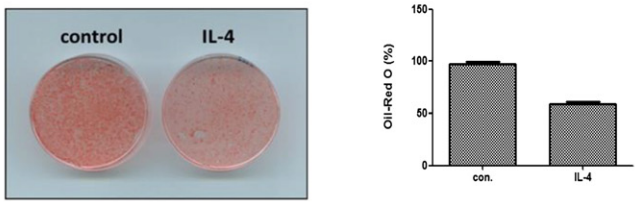
control
IL-4
Oil-Red O (%)
con.
IL-4

(C)

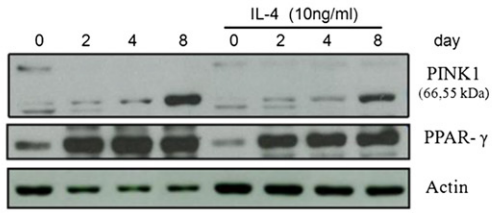
IL-4 (10ng/ml)
0 2 4 8 0 2 4 8 day
PINK1
(66,55 kDa)
PPAR-γ
Actin

(D)

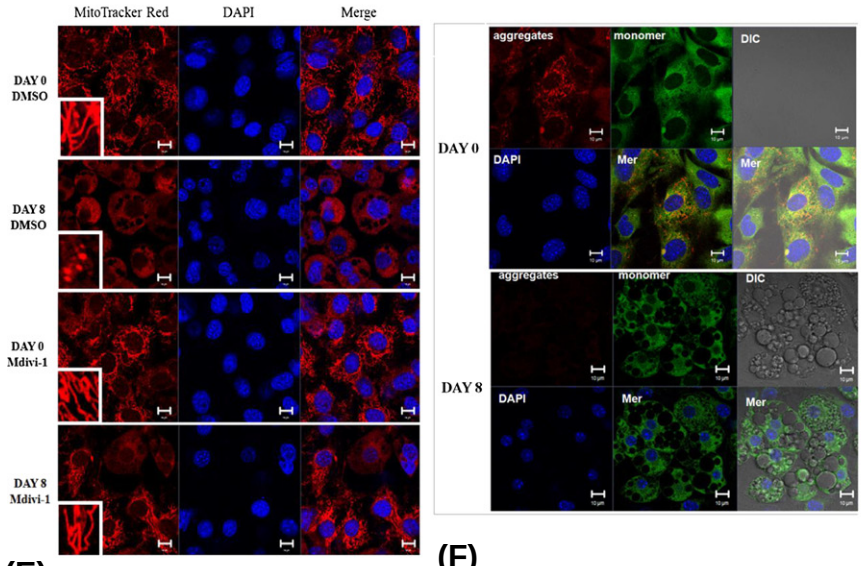
MitoTracker Red
DAPI
Merge
DAY 0 DMSO
DAY 8 DMSO
DAY 0 Mdivi-1
DAY 8 Mdivi-1
aggregates
monomer
DIC
DAPI
Mer

(E) (F)

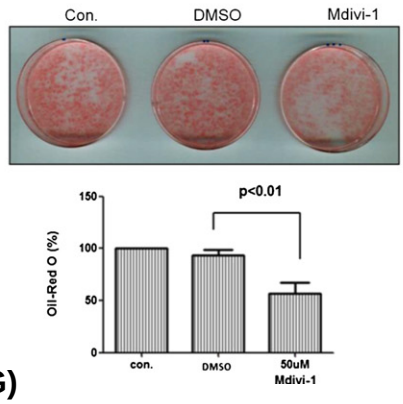
Con.
DMSO
Mdivi-1
p<0.01
Oil-Red O (%)
con.
DMSO
50uM Mdivi-1

(G)

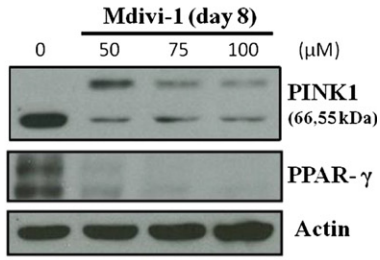
Mdivi-1 (day 8)
0 50 75 100 (μM)
PINK1
(66,55kDa)
PPAR-γ
Actin

(H)

t-test or one-way ANOVA using SPSS software. Statistical difference was defined as $p < 0.05$ for all tests.

3. Results

3.1. PINK1 Undergoes Proteolysis During Adipogenesis

PINK1 expression was temporally examined during the differentiation process of 3T3-L1 pre-adipocytes to evaluate the roles of PINK1 in adipogenesis. Important genes mediating adipogenesis, including CCAAT/enhancer binding protein-α (C/EBPα), peroxisome proliferator-activated receptor-γ (PPARγ) and FABP4, were also analyzed. PINK1 mRNA was significantly increased about 2 folds in the differentiated cells (Fig. 1A). Intriguingly, full-length PINK1 (f-PINK1, 66 kDa) was detected in pre-adipocytes (day 0) but barely detectable after day 2; while smaller PINK1 fragments (s-PINK1, 55 kDa) were increasing along with the differentiation (Fig. 1B). The results suggest that f-PINK1 may undergo proteolysis to smaller fragments which are then accumulated during adipogenesis.

The above data imply that PINK1 proteolysis is coupled to adipogenesis. Therefore, PINK1 processing is likely to be abolished once the differentiation is blocked. Interleukin-4 (IL-4) is known to promote insulin sensitivity and suppresses adipocyte differentiation [22,23], we then tested if PINK1 processing was reversed by IL-4 treatment. Lipid contents were reduced about 40% (Fig. 1C) and PPARγ (Fig. 1D) was also decreased under IL-4 exposure. Notably, f-PINK1 was detectable on day 8 and s-PINK1 fragments were decreased in the presence of IL-4. It suggests that inhibiting adipogenesis hampers PINK1 proteolysis. Therefore, PINK1 expression pattern is coupled with the process of adipocyte differentiation.

3.2. Coupling of Mitochondria Dynamics and PINK1 Alterations in Adipogenesis

We next examined the alterations of mitochondrial morphology for exploring the correlation between PINK1 expression pattern and mitochondrial dynamics in adipogenesis. Microscopic images revealed that the initial filamentous mitochondria on day 0 turned into puncta on day 8 (upper panel, Fig. 1E), with their numbers and membrane potential remarkably decreased in mature adipocytes (Fig. 1F). The results indicate that mitochondria undergo dramatic changes from high-membrane potential filamentous network in pre-adipocytes to fragmented forms with low membrane potential and declined mass in mature adipocytes.

We subsequently examined the possible coupling of mitochondrial alterations and PINK1 expression pattern during adipogenesis in the presence of mitochondria fission inhibitor, Mdivi-1 [24]. Most of the mitochondria on day 8 remained filamentous morphology when mitochondrial fission was repressed by Mdivi-1 exposure (lower panel, Fig. 1E). The lipid contents in Mdivi-1-treated cells decreased about 50% (Fig. 1G). Therefore, differentiation is suppressed once mitochondrial mass cannot be reduced by fission. Meanwhile, PINK1 expression pattern was also reversed by Mdivi-1: f-PINK1 was accumulated and s-PINK1 was markedly decreased under Mdivi-1 exposure (Fig. 1H). Accordingly, PINK1 processing and mitochondrial fission are coupled each other, which is required for pre-adipocytes to fully differentiate into mature adipocytes.

3.3. Autophagy Activity is Decreasing in Adipogenesis

Autophagy is important for cell to keep survive under unfavorable conditions [25]. In the late stage of autophagy, LC3B-II accumulates at the surface of autophagosome to execute autophagic activity for clearing damaged and/or dysfunctional organelles [26]. Autophagy is also implicated in adipogenesis since differentiation is disrupted in autophagy-deficient pre-adipocytes. We next analyzed if temporal alteration(s) of autophagy activity was involved in adipogenesis.

Both LC3B-II/LC3B-1 ratio and Atg14 were significantly decreasing during adipogenic process (Fig. 2A), which were reversed by Mdivi-1 treatment (Fig. 2B). LC3B-II was abundantly dispersed in cytoplasm and co-localized with the filamentous mitochondria on day 0 (Fig. 2C), whereas, it was significantly decreased on day 8. It indicates that although autophagy is highly active in cells under the pressure of confluency before the initiation of adipogenesis, it is rapidly down-regulated once the cells are released from confluency and allowed to differentiate. In addition, autophagy activity is decreasing accompanied with the progression of differentiation.

3.4. PARL-Mediated PINK1 Processing in Early Stage is Required for Adipogenesis

PINK1 is extensively studied in neural cells based on it association to PD. Under normal condition, PINK1 is cleaved by mitochondrial protease presenilin-associated rhomboid-like protein (PARL) [27], then translocated to cytoplasm and targeted

Fig. 1 – Coupling of PINK1 expression and mitochondria dynamics in adipogenesis. 3T3-L1 pre-adipocytes were allowed to undergo differentiation, then PINK1 expression and adipogenesis efficiency were analyzed. (A) Total RNA was isolated from 3T3-L1 cells on day 0 (undifferentiated) and day 8 (differentiated). PINK1 mRNA was analyzed by real-time PCR. Gene expression was normalized to 18s rRNA. (B) PINK1, Parkin and adipogenic markers were examined by Western blotting at the timed indicated during differentiation. (C) Cells were induced into mature adipocytes in the absence (control) or presence of IL-4 (10 ng/ml) treatment and subjected to Oil-Red O staining (left panel). Quantification of Oil-Red O staining results was shown in the right panel. (D) Western blotting analysis showing the patterns of PINK1 and PPARγ expression during 3T3-L1 differentiation. (E) Mitochondrial morphology of cells at day 0 and 8 in the absence (DMSO) or presence of Midvi-1 was examined by confocal microscopy with mitotracker red staining. The inserts were the enlarged images showing mitochondria morphology. (F) Mitochondrial membrane potential during adipogenesis was analyzed using the cationic fluorescent dye JC-1 (5 μM). The monomer JC-1 showed green fluorescence (loss membrane potential), while the aggregates showed red fluorescence (normal membrane potential). Nucleus was labeled using DAPI (blue), scale bar represent 10 um. The morphological alternations were disrupted by Mdivi-1. (G–H) Adipogenesis and PINK1 proteolysis were attenuated by Mdivi-1.

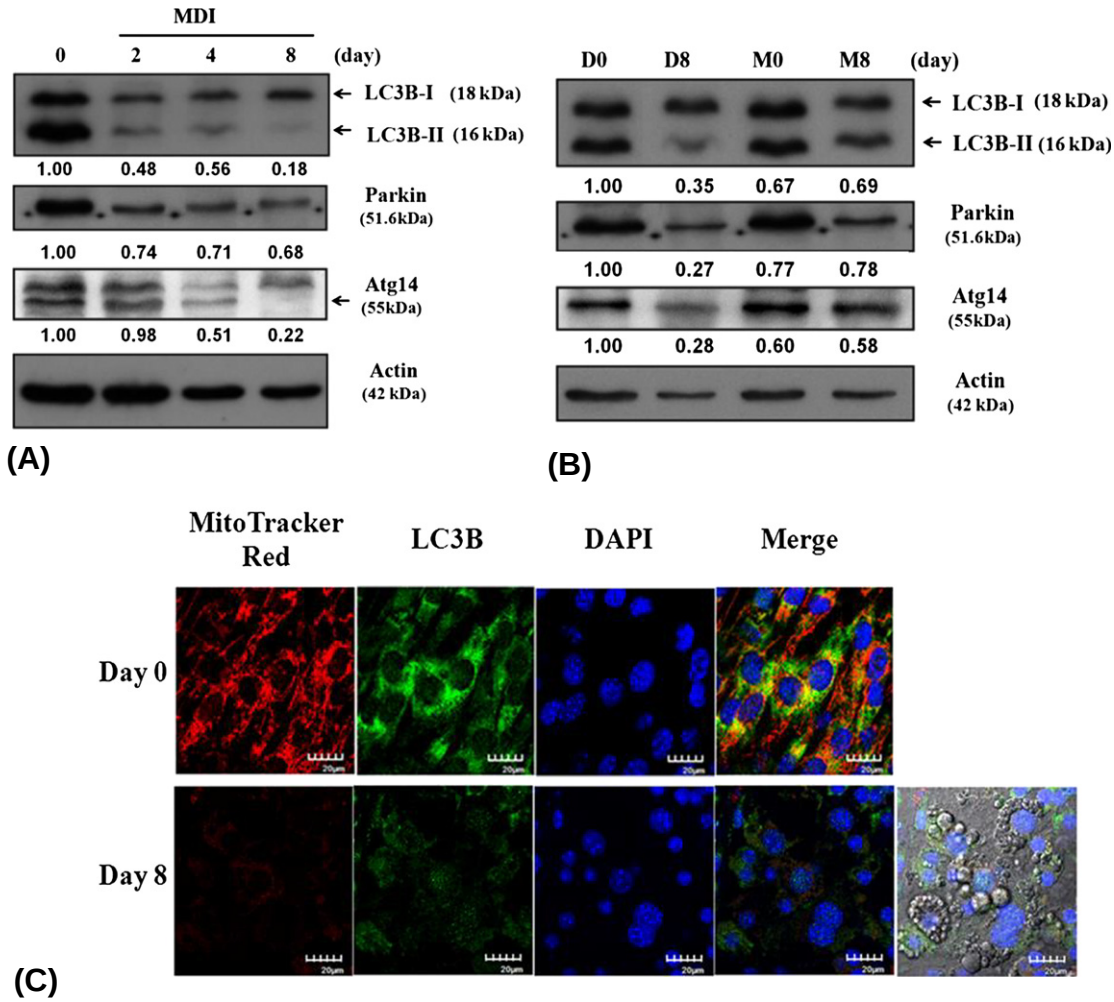

Fig. 2 – Autophagy activity is decreasing in adipogenesis. (A) Cells were induced into differentiation, Parkin, LC3B and Atg14 were examined by Western blotting at the timed indicated during differentiation. (B) The decrease of Parkin, LC3B and Atg14 on day 8 (D8) were attenuated by Mdivi-1 (M8). Intensity of bands was quantified and presented as a ratio to Actin, with day 0 cells as 1. (C) Immunofluorescent images showed the mitochondria morphology (red, stained by MitoTracker Red) and distribution of LC3B in undifferentiated and differentiated 3T3-L1 cells. Nucleus was labeled using DAPI (blue), scale bar represent 20 um. The right picture of the second row was phase contrast image.

for degradation by proteasome [11]. In mitochondria with low membrane potential, PINK1 recruits Parkin to mediate mitophagy for eliminating dysfunctional/damaged mitochondria [28–30]. It was of interest for us to investigate if the scenario of PARL-PINK1-Parkin system in controlling mitochondrial dynamics of neural cells was applied to adipocyte differentiation.

PARL mRNA and protein were significantly increasing along with the differentiation (Fig. 3 A&B); intriguingly, the decreased f-PINK1 on day 2 coincided with the increased PARL (Fig. 3C). The temporal alterations of PARL and PINK were inhibited by Mdivi-1, with f-PINK1 remained detected on day 8 (Fig. 3C). It suggests that PINK1 is processed by PARL in pre-adipocytes. Furthermore, PARL-PINK1 association was detected in day 0–4 (Fig. 3D). It supports that f-PINK1 is cleaved by PARL in mitochondria at the early phase, and the produced s-PINK1 then accumulates during adipogenesis (Figs. 1B & 3C).

To further verify the roles of PARL-PINK1 interaction in adipogenesis, adipogenic efficiency, PINK1 alternations and mitochondria depletion were temporally analyzed by PARL knockdown. When PARL expression was successfully inhibited (Fig. 3E), alterations of PINK1 expression were apparently blocked (Fig. 3F). Notably, f-PINK1 was detected throughout the entire process and only trace amounts of s-PINK1 were generated. PPARγ, C/EBPα and FABP4 were almost entirely inhibited (Fig. 3F), leading to nearly aborted adipogenesis (Fig. 3G). The above results reveal that f-PINK1 processing by PARL in mitochondria is required for adipogenesis.

Additionally, the expression of PARL and PINK1 was temporally examined both in the pre-adipocytes undergoing differentiation (0–8 day) and in mature adipocytes (8–12 day). PARL and s-PINK1 were increasing in the adipogenic process and remained high-level expression in mature adipocytes (Fig. 3H). The mitochondria fragmentation-mediated dynamin-

related protein-1 (Drp1) [31] was also increasing accompanied with the progression of adipogenesis and remained at high level in mature adipocytes (Fig. 3H). The results suggest that, in addition to be required for adipocyte differentiation, PARL and Drp1 are necessary to maintain low mitochondrial mass in mature adipocytes for ensuring minimal energy consumption.

3.5. PARL-Processed PINK1 Mediates Parkin Degradation in Late Adipogenesis

In contrary to PARL and PINK1 alterations, levels of Parkin were peaked on day 0 and gradually decreasing during differentiation (Figs. 1B and 3C). The decreasing Parkin expression pattern was suppressed by Mdivi-1 (Fig. 3C) and abolished by PARL silencing (Fig. 3F).

The subcellular distribution of PINK1 and Parkin were subsequently investigated. Parkin mainly localized in cytosol throughout the differentiation, only trace amount of Parkin was detected in mitochondria on day 0 (Fig. 4A). Meanwhile, f-PINK1 was detected in mitochondria on day 0, and s-PINK1 was increasing in both cytosol and mitochondria (Fig. 4A). Notably, reciprocal alteration of s-PINK1 and Parkin in cytosol was identified. It implies that after being processed by PARL during day 0–4, s-PINK1 translocates and accumulates in cytoplasm. The increasing s-PINK1 is correlated to the decreasing Parkin during adipogenesis.

Next, PINK1 and Parkin interaction was analyzed by co-immuoprecipitation. Fig. 4B showed that s-PINK1 was associated with Parkin during the late stage of differentiation. Notably, a laddering Parkin signal was detected, which implied that the precipitated Parkin was conjugated with ubiquitin (Ub). Therefore, whether Parkin was ubiquitinated (Ub-) during adipogenesis was tested to verify this speculation. Ub-proteins were first immunoprecipitated in the presence or absence of MG132, followed by probing PINK1, Parkin or Ub with immunoblotting. Fig. 4C indicated that the Ub-proteins were first diminished at early stage (0–4 day), then rapidly increasing and peaked on day 6. Both s-PINK1 and Parkin were ubiquitinated. Particularly, Ub-Parkin was greatly increased during differentiation while MG132 inhibited the decreasing of Parkin (Fig. 4D), which indicated that Ub-Parkin was degraded by proteosome.

Taking the above data together (Fig. 4E), we suggest that the increased PARL interacts with and cleaves f-PINK1 at early stage (day 0–4). Then the proteolytic s-PINK1 translocates from mitochondria to cytoplasm, accumulates and associates with Parkin at late stage (after day 4). The PINK1-Parkin complex is ubiquitinated, leading to Parkin degradation by proteosome. Given that Parkin degradation inhibits mitophagy, we suggest that mitophagy activity is gradually reduced at late stage of differentiation. Notably, PARL knockdown blocks PPARγ and aborts adipogenesis. Therefore, the PARL-PINK1-Parkin system is required to ensure the proceeding of adipogenesis.

3.6. GSK-3β Induced Drp1-Mediated Mitochondrial Fission in Late Adipogenesis

PINK1 and Parkin mutations result in mitophagy deficiency and elevated Drp1 expression [31]. Recent evidence suggests that Drp1 is activated by GSK-3β, therefore, we inferred that Drp1 may be up-regulated by PINK1-dependent Parkin degradation at late stage of adipogenesis. Accordingly, the expression of Drp1 and its regulating molecules, including Akt and GSK-3β, was investigated.

Fig. 5A showed that p-Akt was decreasing while p-GSK-3β was increased at early stage, peaked on day 4 then decreasing thereafter. Drp1 was significantly increasing since day 4, whereas, the major mitochondria fusion effector mitofusion-1 (MFN1) was increasing during day 0–4 then decreased. Microscopic images showed that mitochondria mass was increased during day 0–4 probably due to MFN1 mediated-elongation, then Drp1 was abundantly dispersed in cytoplasm and co-localized with mitochondria after day 4 to mediate mitochondrial fragmentation (Fig. 5B). Therefore, the filamentous mitochondria network turned into puncta in day 5–6, with most of them cleared on day 8. Interestingly, the increasing Drp1 during adipogenesis was also abolished by PARL shRNA (Fig. 3F). Furthermore, the expression pattern of p-Akt, p-GSK-3β and Drp1 (Fig. 5C), as well as the mitochondrial phenotype (Fig. 5D) were all attenuated by Mdivi-1 by which the mitochondrial fission was impaired. The above results indicate that Drp-1-mediated mitochondrial fission is critical and required for adipocyte differentiation.

The above data indicate that GSK-3β activity is up-regulated after day 4 when p-Akt is decreased, which corresponds to the timeframe of Parkin degradation, MFN and Drp1 alterations, and mitochondrial morphological changes during adipogenesis. All the identified sequential events and finely-tuned machinery are disturbed once the adipogenesis is hindered by Mdivi-1 or blocked by PARL shRNA.

3.7. Alteration of Energy Metabolism During Adipogenesis

The major function of adipocytes is the body energy reservoir. As mitochondrial mass is greatly diminished by GSK-3β-activated Drp1-mediated fission at late adipogenic stage, it was intriguing to monitor cellular glucose uptake ability for elucidating metabolic alterations during adipogenic process. Under the control condition, the insulin-triggered glucose uptake was peaked on day 4 and decreased thereafter at late stage (DMSO INS, Fig. 6A). In the presence of Mdivi-1, glucose uptake also peaked on day 4 but remained high until day 8 (Mdivi-1 INS, Fig. 6A). During adipose differentiation, GLUT4 is progressively expressed while GLUT1 shows no apparent change [32]. Accordingly, difference between the measures of Mock and INS treatments was estimated to analyze the GLUT4-specific glucose uptake triggered by insulin. In parallel to the total amounts of glucose uptake in Fig. 6A, the alterations of insulin-dependent GLUT4-responsible glucose uptake in adipogenesis was also peaked on day 4, and decreased thereafter (Fig. 6B). Likewise, the markedly reduced GLUT4-specific glucose uptake was attenuated by Mdivi-1 exposure (Fig. 6C).

The intracellular ATP contents were also measured to monitor energy status during adipogenesis. In consistent with the glucose uptake ability and mitochondrial dynamics, ATP contents was increasing at early stage (day 0–4), and plunged at the late stage to minimal levels on day 8 (DMSO, Fig. 6D). As anticipated, the decreasing ATP contents at late stage were sequestered by Mdivi-1 (DMSO, Fig. 6D).

These results demonstrate that mitochondrial changes are coordinated with glucose uptake ability and ATP contents

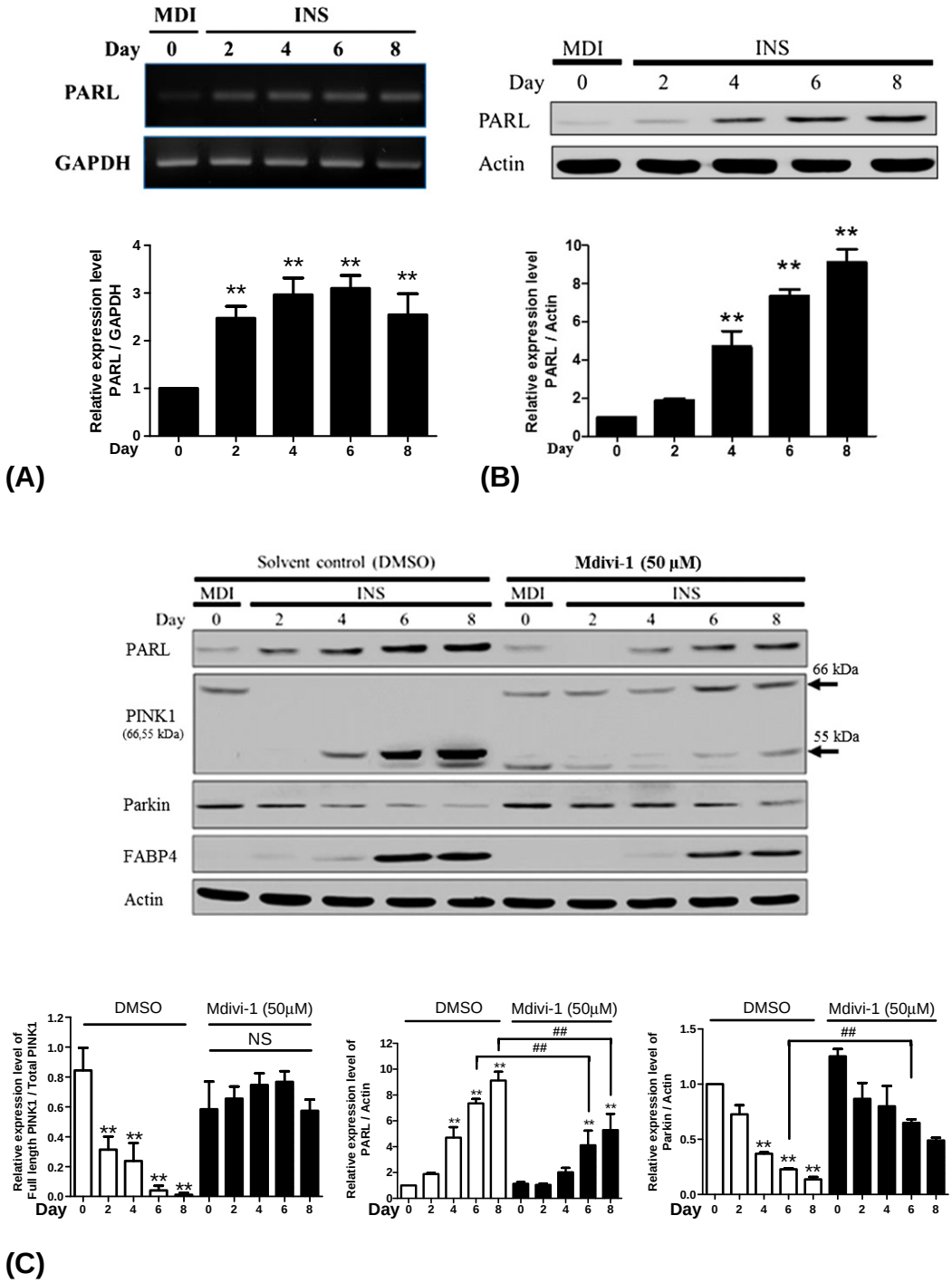

Fig. 3 – PARL-mediated PINK1 processing is required for adipogenesis. Cells were induced into differentiation, then expression of PARL, PINK1, Parkin and adipogenesis efficiency was analyzed at the time indicated. PARL mRNA (A) and protein (B) were increasing in differentiation. $^{**}p < 0.05$ vs. day 0. (C) Alterations of PARL, PINK1, Parkin and FABP4 during adipogenesis were attenuated by Mdivi-1. $^{**}p < 0.05$ vs. day 0, $^{\#\#}p < 0.05$, between the groups indicated. (D) Interaction between PARL and PINK1 in mitochondrial extracts. Mitochondrial proteins were immune-precipitated with PINK1 (upper panel) or PARL (lower panel) Abs at the time indicated, followed by immunoblotting using either PARL or PINK1 Abs. (E) PARL was successfully knocked down by shRNA. (F–G) Effects of PARL silencing on expression of PINK1, Parkin, Drp1, adipogenic markers and adipogenesis efficiency. For (E) and (G), $^{**}p < 0.05$ vs. control. (H) Expression of PARL, PINK1 and Drp1 in 3 T3-L1 cells was analyzed at the time indicated during adipogenesis (0–8 day) and the terminal differentiated mature adipocytes (8–12 day).

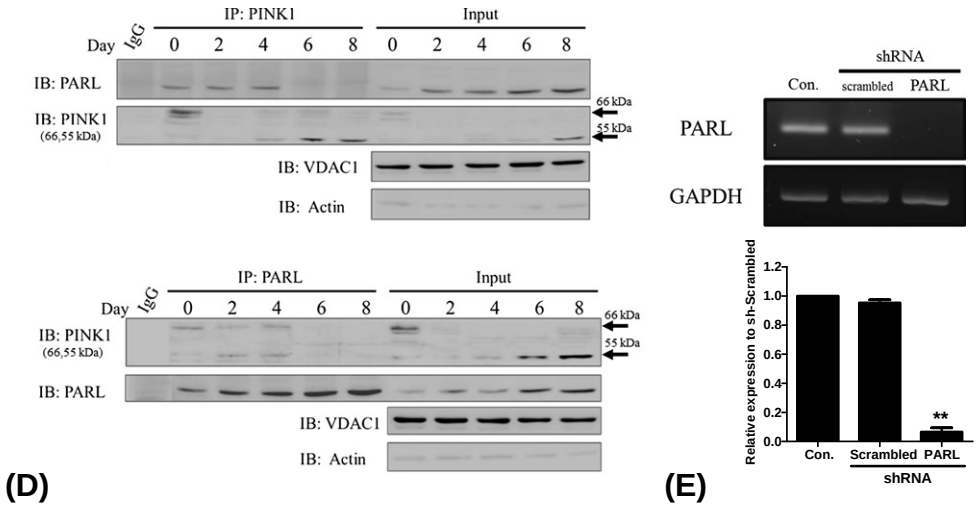

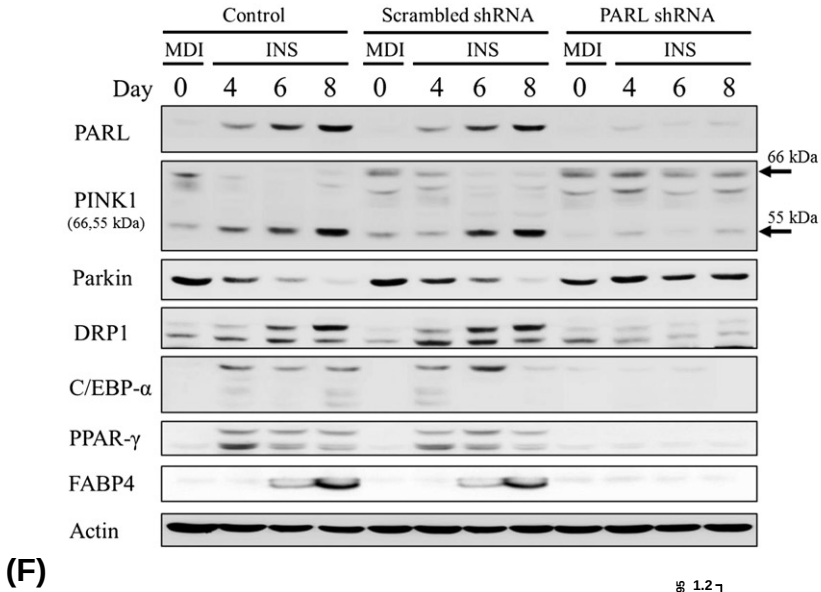

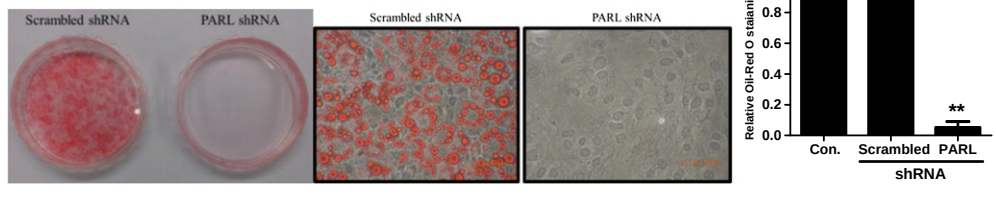

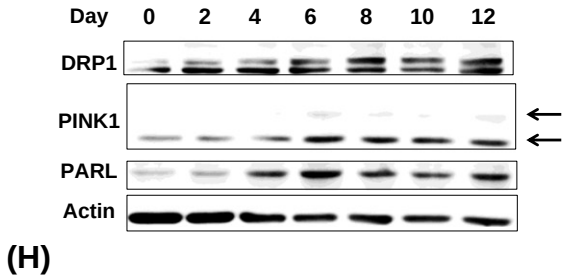

Fig. 3 (*continued*).

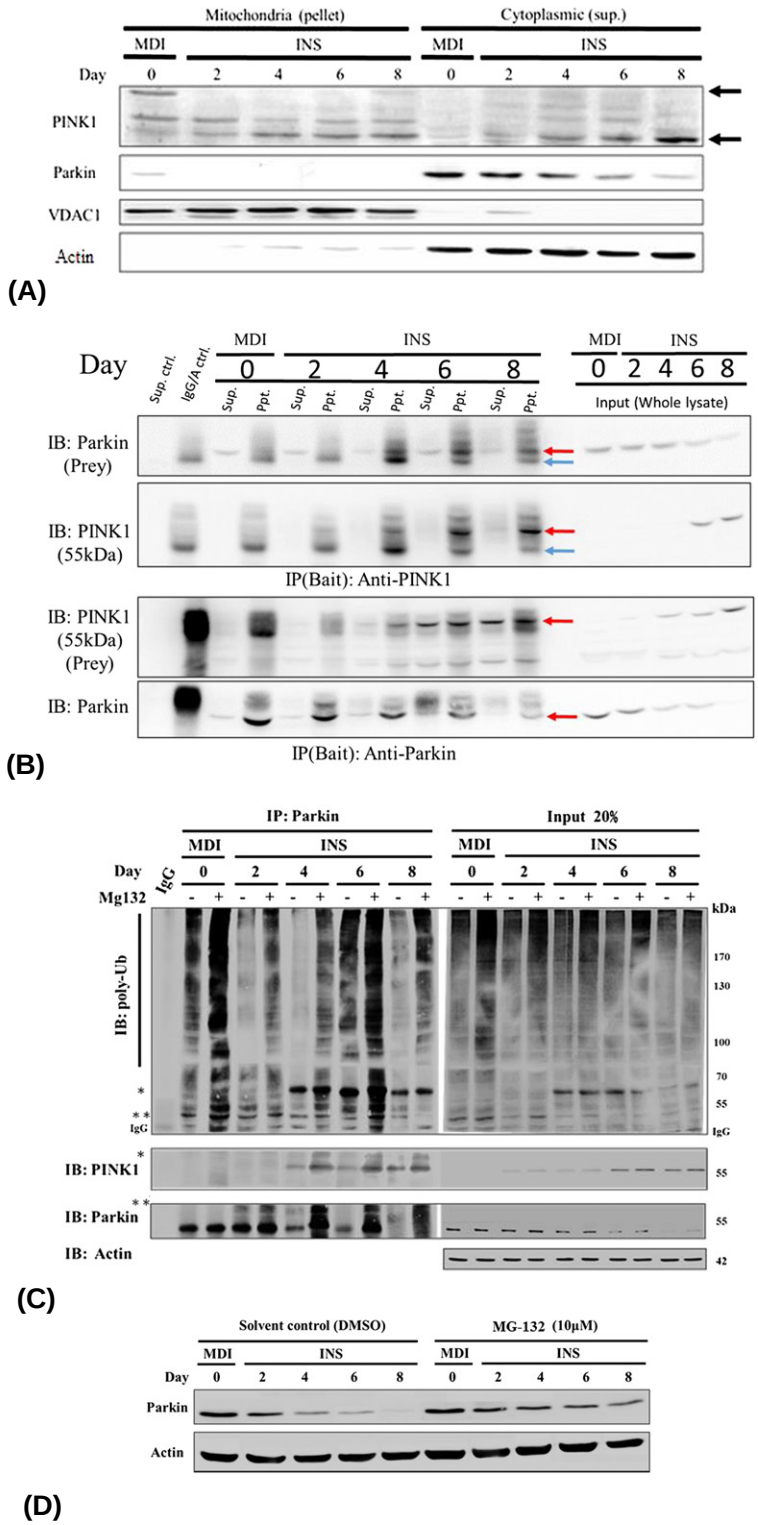

Fig. 4 – Interaction between PINK1 and Parkin in adipogenesis.Cells were induced into differentiation, then interaction between PINK1 and Parkin was analyzed at the time indicated. (A) PINK1 and Parkin were respectively probed in mitochondrial and cytoplasm fraction. (B) Interaction between PINK1 and Parkin was analyzed by co-immunoprecipitation. Cell lysate was immune-precipitated with PINK1 (upper panel) or Parkin (lower panel) Abs, followed by immunoblotting with either Parkin or PINK1 Abs. Red and blue arrow indicates the specific binding and the heavy chain of the immunoblotting in each panel, respectively. (C) Cell lysates with or without 6 h exposure to 5 μg/mL MG132 were immune-precipitated with Parkin Abs, followed by immunoblotting using ubiquitin (Ub), PINK1 (·) or Parkin (··) Abs. (D) Parkin in cell lysates collected as in (C) was analyzed by immunoblotting. (E) PARL is increasing and responsible for PINK1 cleavage during adipogenesis. The proteolytic PINK1 fragments are released to cytosol and associated with Parkin, which result in Parkin degradation.

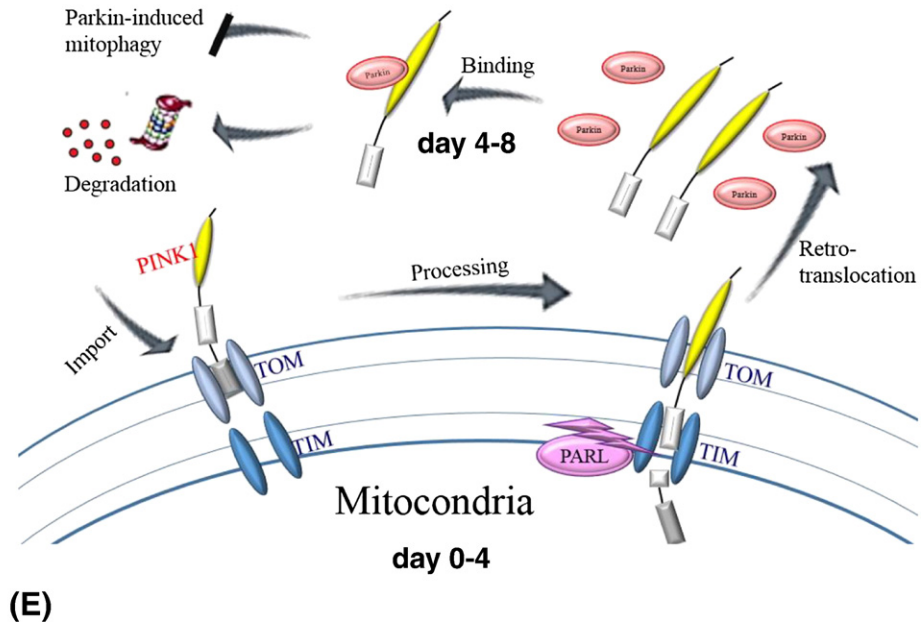

Fig. 4 (*continued*).

during adipogenesis. Collectively, we suggest that the alterations of energy metabolism pattern during adipogenesis aim to minimize energy consumption for achieving the morphological and functional characteristics of mature adipocytes.

3.8. *PARL and PINK1 Expression are Correlated With Obese and Diabetic Status*

We next examined the in vivo expression profile of Drp1, PARL and PINK1 to probe possible correlation between these proteins with obesity and diabetes. Epididymal adipose tissues were harvested from diet-induced obese (HFD) mice, genetic-deficiency obese mice (*ob/ob* and *db/db*), and diabetic mice (HFD + STZ). The results showed that f-PINK1 was only faintly probed in WT mice (Fig. 7), and expression profiles of PARL and s-PINK1 were very similar. Interestingly, PARL and s-PINK1 were greatly decreased in all the obese mice models while they were highly expressed in diabetic HFD + STZ mice. No significant difference of Drp1 levels among mice groups was observed although the Drp1 was relatively higher in HFD + STZ mice.

These data strongly suggest that PARL and PINK1 are not only correlated with obesity, but also very likely participate in the diabetic pathogenesis and progression.

4. Discussion

Understanding adipogenesis is increasingly important as adipogenesis determines the adipose reservoir which modulates body energy metabolism through adipokines. It is feasible to develop adipogenesis-intervening strategies for manipulating whole-body energy intake/expenditure to cope with the obesity epidemics. Although the participation of PINK1-Parkin in maintaining mitochondrial homeostasis in neural cells and its association with PD are extensively elucidated, the molecular events behind mitochondrial dynamics during adipogenesis have never been revealed. In this context, it is of great interest for us to explore the PARL-PINK1-Parkin workflow and mitochondrial remodeling during adipogenesis. Our results uncover that PARL-PINK1-Parkin system is required for successful proceeding of physiological adipocyte differentiation.

A PARL-PINK1-Parkin working model in adipogenesis is proposed (Fig. 8A). First of all, the pre-adipocytes facing confluency stress may undergo autophagy before the initiation of adipogenesis. The entire adipogenic process is dissected into 3 stages according to the participation of PARL-PINK1-Parkin system. (1) Once the cells are released from confluency and switched to differentiation, f-PINK1 is subjected to PARL cleavage to generate s-PINK1 at early stage of differentiation (0–4 day). Increasing PARL cleavage events lead to s-PINK1 accumulation in mitochondria. At this stage, mitochondrial mass is increased probably due to MFN1-mediated elongation for generating ambient energy to meet the demands for cellular remodeling. (2) At the second stage of adipogenesis (5–6 day), s-PINK1 persistently accumulates in mitochondria and translocates into cytoplasm to mediate Parkin degradation. Mitochondria are fragmented by Drp1-mediated fission, and cleared by autophagy to reduce their mass. (3) At the late stage of adipogenesis (7–8 day), only residual autophagy is remained when most of mitochondria have been eliminated. In addition, the expression of PARL and Drp1 remain high in the terminal differentiated adipocytes, which may aim at maintaining low

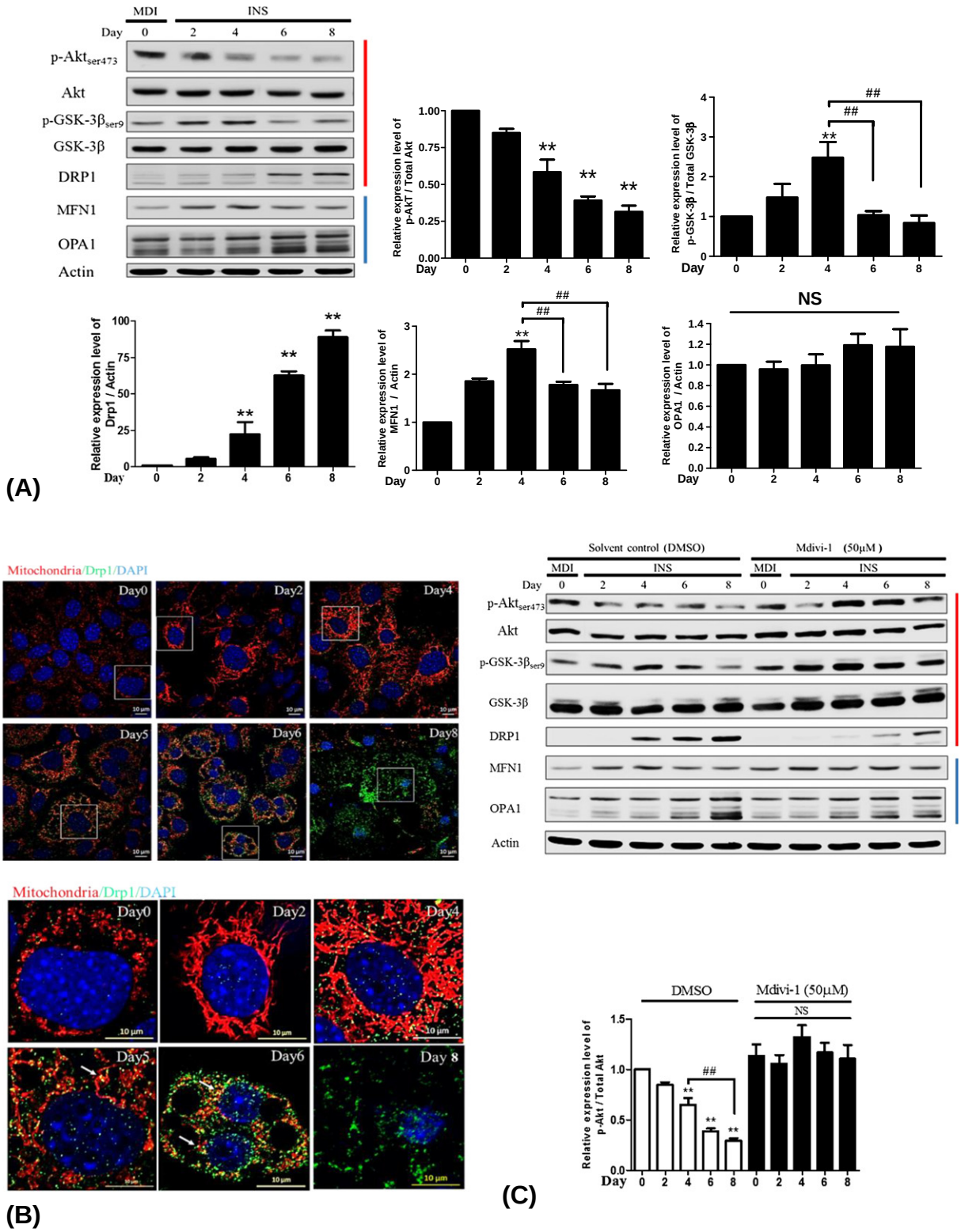

Fig. 5 – GSK-3β induces Drp1-mediated mitochondrial fission in late adipogenesis. Cells were induced into differentiation, with molecules mediating mitochondria dynamics analyzed. Mitochondrial fission protein p-Akt, p-GSK-3β, and Drp1, and fusion proteins MFN1 and Opa1, were analyzed in the time indicated without (A) or with Mdivi-1 treatment (C). Red and blue line at the right of figures indicated proteins related to mitochondria fission and fusion, respectively. $^{**}p < 0.05$ vs. day 0, $^{\#\#}p < 0.05$, between the groups indicated. Drp1 expression and distribution (green), in the absence (B) or presence of Mdivi-1 (D), were analyzed by immunofluorescence staining. Images in lower panel of (B) showed the corresponding enlarged one of the area labeled in upper panel. Nucleus was labeled using DAPI (blue), scale bar represent 10 um.

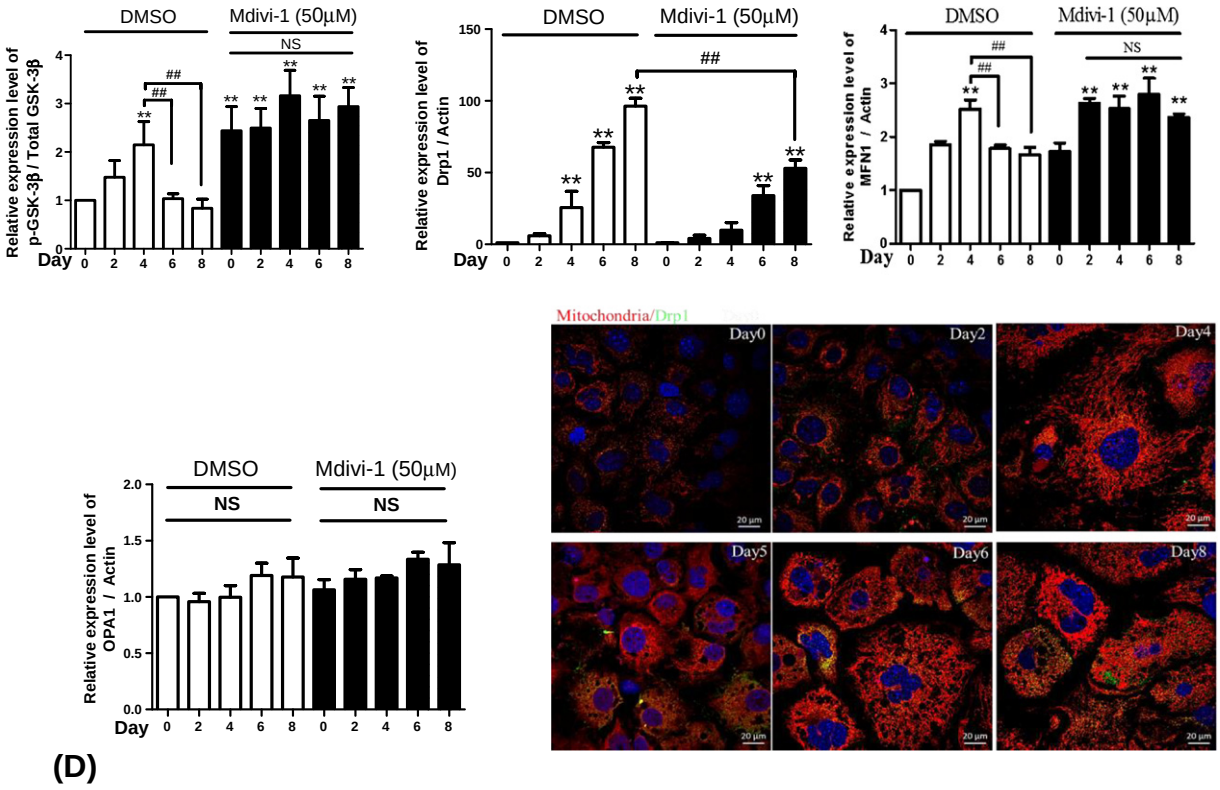

Fig. 5 (*continued*).

mitochondrial mass in mature adipocytes. The mitochondria clearance and high-level PARL/Drp1 expression maintain energy consumption of mature adipocytes at the minimal levels for storing energy.

Hence, the operation of PARL-PINK1-Parkin system is coordinated with mitochondrial changes and energy metabolism during adipogenesis. We suggest that excess mitochondria are subjected to Drp1-mediated fission and cleared by autophagy, with only residual autophagy activity remaining in late stage of differentiation. Interestingly, PARL-silencing inhibits PPARγ and aborts adipogenesis, which demonstrates the pivotal role of PARL-PINK1-Parkin system in adipogenesis.

PARL is identified as a candidate gene for insulin resistance and T2DM [33], its genetic variation contributes to earlier diabetic onset and increased susceptibility to diabetic complications. However, whether PARL is associated with T2DM is still controversial with conflicting results [34]. Our results support and may elucidate the rationale for PARL as T2DM susceptible gene since PARL may determine, at least in part, the mass of adipose reservoir which is correlated with obesity. Particularly, our animal study results show significant correlation between PARL and the diabetic status (Fig. 7), which strongly suggests that PARL-PINK1-Parkin system participate in diabetic pathogenesis and/or disease progression.

The results regarding lower levels of PARL and PINK1 in adipose tissue from obese animal models (Fig. 7) seem to be contradictory to the higher PARL and PINK1 expression in mature adipocytes (Fig. 3H). We suggest that the differential status of adipocytes in the cell and animal model should be able to explain these observations. In cell model, the alterations and profiles of PARL-PINK1-Parkin are continuously monitored to illustrate the participation of the system in the entire process of adipocyte differentiation model. Whereas, in animal model, PARL and PINK1 levels represent the cross-sectional outcome after the animals have become obese with long-term HFD or diabetic onset. Therefore, results from the cell model demonstrate the involvement of PARL-PINK1-Parkin in the progression of adipocyte differentiation, while the animal data reflect the events in the expanded and enlarged adipose tissues. Notably, the findings that PARL is significantly correlated with obese and diabetic status provide strong molecular evidence deciphering the previous report that PARL is a candidate gene for insulin resistance and T2DM [33].

The present study provides another evidence of PARL-PINK1-Parkin system regulating mitochondrial dynamics and glucose metabolism through insulin signaling. PINK1 is identified as a target gene activated by tumor suppressor phosphate and tensin homologue deleted on chromosome 10 (PTEN) [35]. PTEN down-regulates PI3K functions for activating Akt, and thereby modulates insulin signaling and glucose metabolism [15,16]. The activation of GSK-3β by PARL-PINK1-Parkin system in our study echoes the previous report that suppressing PARL in healthy myotubes lowers mitochondrial mass and insulin-stimulated glycogen synthesis [36]. Given Parkin is the downstream effector of PINK1, it is logical that PARL-PINK1-Parkin system also functions through PI3K/Akt signaling pathway.

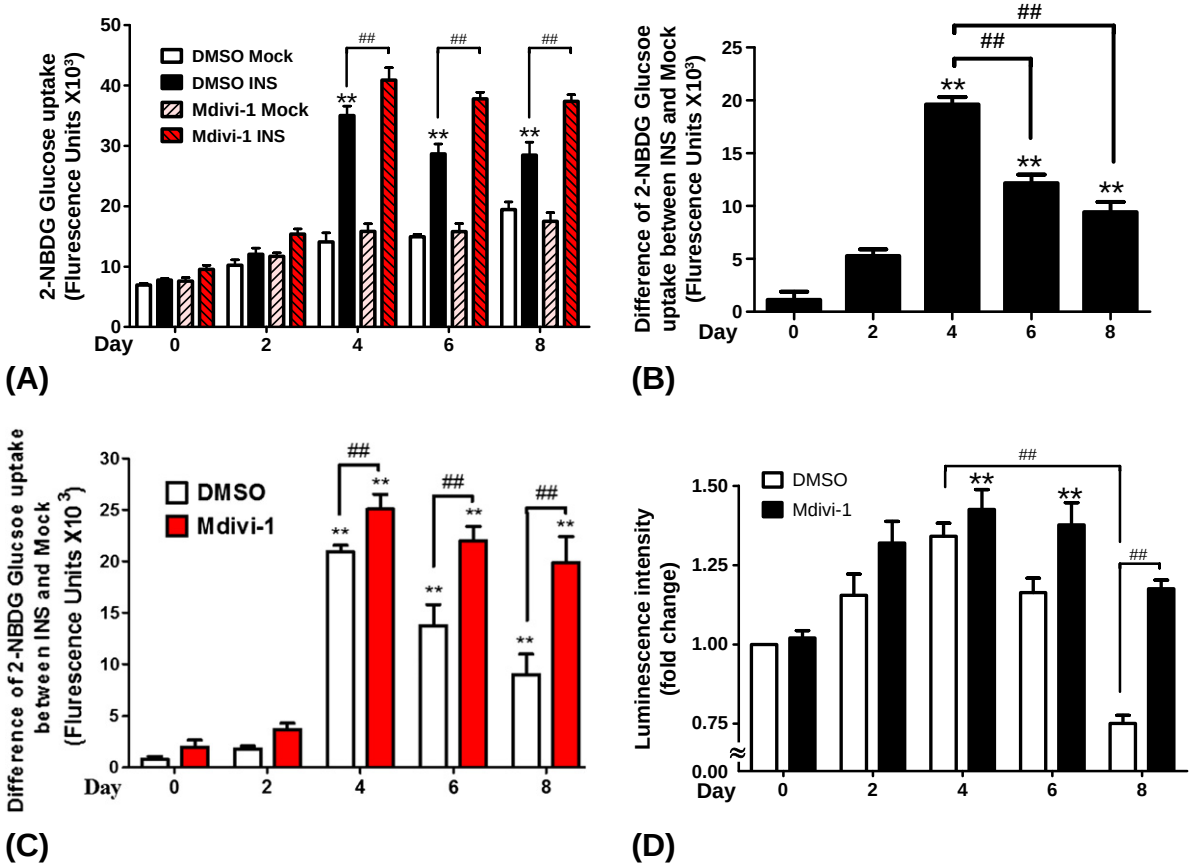

Fig. 6 – Alterations of energy metabolism during adipogenesis. Cells were induced into differentiation, with glucose uptake ability and ATP content analyzed at the time indicated. (A) Glucose uptake ability during adipogenesis without (DMSO) or with Mdivi-1 exposure was assessed. Y-axis represents the measures of 2-NBDG fluorescence. (B and C) Insulin-dependent GLUT4 glucose uptake in the absence (B) or presence (C) of Mdivi-1 was shown by the difference of 2-NBDG measures between INS and Mock. (D) ATP content was examined by luminescence. $^{**}p < 0.05$ vs. DMSO INS on day 0; $^{\#\#}p < 0.05$, between the groups indicated.

Accumulating evidence reports the association of mitophagy with metabolic abnormalities in insulin-secreting β-cell, insulin-targeting cells and diabetic complications. Mitochondrial function is impaired during insulin resistance that progresses to metabolic disorder [37–39]. In β-cells, Parkin deficiency leads to lower mitochondrial membrane potential and insulin expression/secretion, while mitochondrial fragmentation and ROS production are increased [40]. Low mitochondrial mass in skeletal muscle is associated with insulin resistance and obesity [41,42]. The study group concludes that skeletal muscle inflexibility plays a major role in causing insulin resistance [43,44]. Our study supports and addresses the underlying mechanism for the finding that mice with mitochondria degradation deficiency exhibit reduced adiposity, resistance to diet-induced obesity, and increased insulin sensitivity [45]. Given our results demonstrating that PARL-PINK1-Parkin system is required for adipogenesis and mediates energy metabolism via Akt-GSK-3β, it is logical to assume that imbalance in mitochondrial dynamics can result in defects associated with energy metabolism and insulin resistance.

This study also agrees with numerous epidemiological and biochemical evidence which indicate a link between T2DM and PD, and may explain the rationale behind. Parkin is suggested to modulate PI3K/Akt pathway in neurons since active Akt is significantly suppressed in heads of Parkin-deficient drosophila [46]. Besides, neurotoxin-induced apoptosis of dopaminergic neurons is prevented by introducing a membrane-targeting constitutively active Akt in brain [47]. Huang et al. recently reported that impaired long-term memory in *db/db* mice is restored by modulating Drp1 through inhibiting GSK3β activity [48], which points to the involvement of mitochondria in diabetes-induced synaptic dysfunction. Additionally, metformin exerts neuro-protective effect on PD via Parkin restoration [49].

Nevertheless, data from this study are not able to fully explain the consistent accumulation of Ub-s-PINK1 at late stage of adipogenesis. PINK1 is known to be rapidly degraded by proteosome after binding to Parkin. We speculate that Hsp90 may stabilize cytosolic s-PINK and lead to PINK1 accumulation at late stage of adipogenesis since stability of cytosolic PINK1 requires chaperone Hsp90 activity [50]. However, this

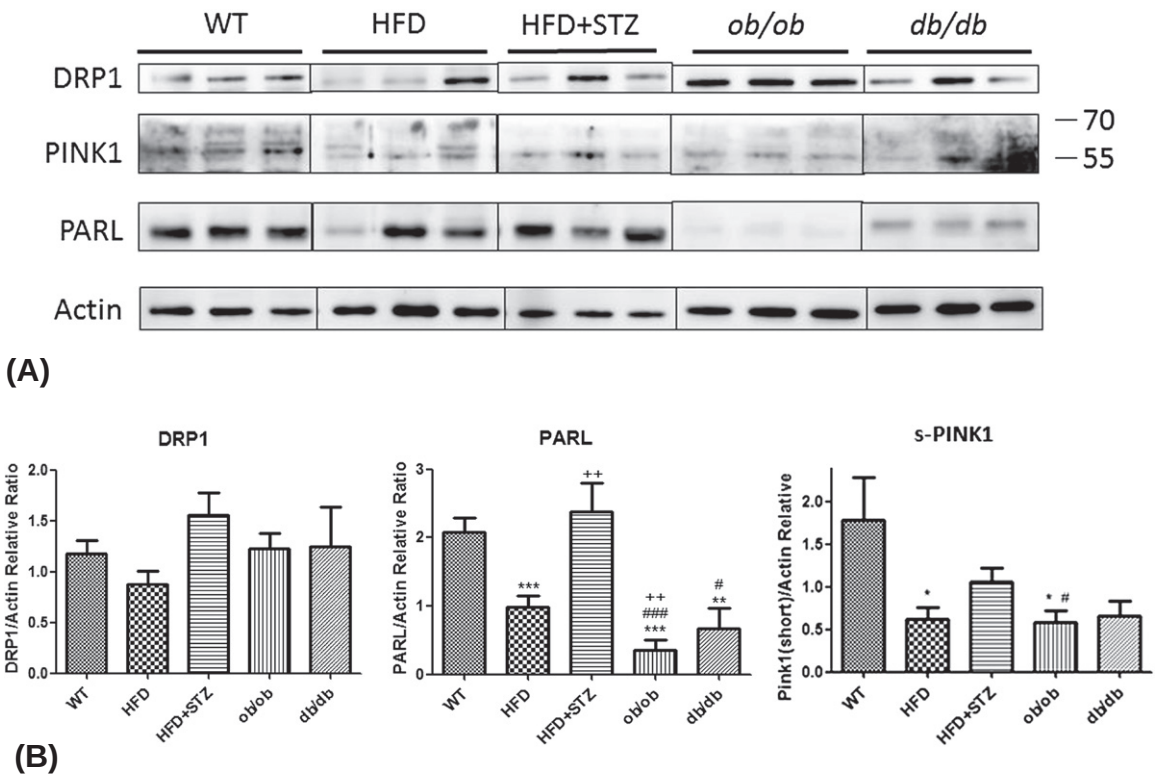

Fig. 7 – Expression of Drp1, PARL and PINK1 in adipose tissues from obese and diabetic mice models. Representative results of Western blot analysis showed the Drp1, PARL and PINK1 expression in epididymal fat tissues obtained from standard Chow diet-feeding WT mice (n = 7), HFD obese mice (n = 5), HFD + STZ diabetic mice (n = 3), *ob/ob*(n = 7) and *db/db*(n = 4) obese mice. $^{*}p < 0.05$ vs. WT; $^{**}p < 0.01$ vs. WT; $^{***}p < 0.001$ vs. WT; $^{\dagger\dagger}p < 0.01$ vs. HFD; $^{\#}p < 0.05$ vs. HFD + STZ; $^{\#\#\#}p < 0.001$ vs. HFD + STZ.

speculation needs further study to confirm. Besides, several putative binding sites of transcriptional factors involved in adipogenesis and metabolism, such as C/EBPα and C/EBPβ, were identified on PINK1 promoter (Fig. 8B, analyzed by TIFBIND). We hypothesized that a subtle loop between adipogenesis and PARL-PINK1-Parkin system may be finely orchestrated for maintaining metabolic homeostasis to meet the changing cellular demands. This clue further supports the convergence between insulin signaling and PARL-PINK1-Parkin system in adipocytes to address the linkage between PD and T2DM comorbidity.

5. Conclusions

This study identifies the novel role of PARL-PINK1-Parkin system in adipogenesis. As obese individuals is susceptible to insulin resistance and multiple metabolic disorders, understanding adipocyte behaviors offers a great opportunity to tackle the obesity associated metabolic abnormalities and disorders. Our findings not only address the sequential events directed by PARL-PINK1-Parkin system in adipogenesis and energy metabolism, but also shed light on the convergence of neurodegenerative and metabolic diseases. Hopefully, this study provides substantial information for supporting the possibility of developing novel therapeutic strategies for neural and/or metabolic diseases by intervening and manipulating the size/reservoir of adipose tissue.

Author Contributions

LPS, HYJ, YCP, SCW, CKY and CHW carried out the cell experiments, data collection and interpretation, and statistical analysis. SMY and CYH conceived the study design and coordination, data interpretation, manuscript drafting, and giving final approval of the manuscript.

Funding

This work was supported by grants from Ministry of Science and Technology (MOST 104–2320-B-010-019 and 105–2320-B-241-005) and Ministry of Education (Aiming for the Top University Plan, 103 AC-P686, 104 AC-P686 and 105 AC-P686), Taipei, Taiwan. We thank the confocal microscopy technical services provided by Imaging Core Facility of Nanotechnology, UST-NYMU.

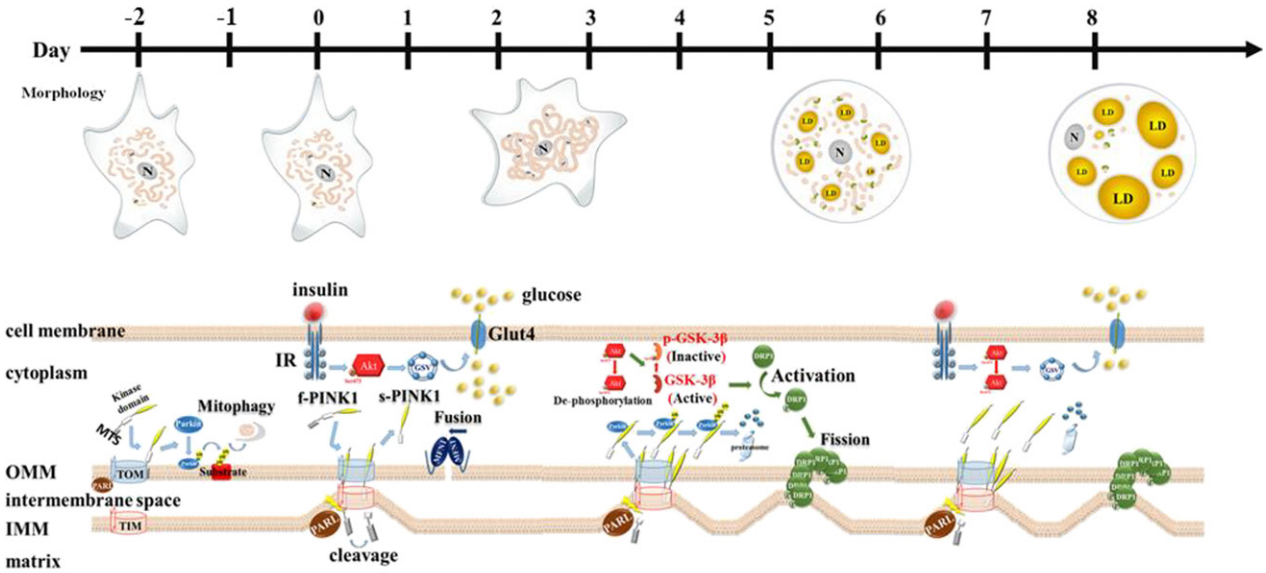

(A)

Putative transcription facctor binding sites within the 5'-adjacent sequence of the PINK1 gene

Transcription factor	Recognition sequence	Localization
CHOP-C/EBP alpha	ACCTGTAATCCCC	-717 to -695
C/EBP beta	GTATTATGTGATTT	-810 to -797
C/EBP alpha	ATTTTACACACACA	-800 to -787
SREBP-1	CAACACCCCCC	-881 to -871

(B)

Fig. 8 – Role of PARL-PINK1-Parkin system in adipocyte differentiation. (A) N, nucleus; LD, lipid droplet; IR, insulin receptor; Glut4, glucose transporter 4; MTS, mitochondria-targeting sequence; TIM, translocase inner membrane; TOM, translocase outer membrane; OMM, outer mitochondrial membrane; IMM, inner mitochondrial membrane. (B) Putative recognition sequences of transcriptional factors involved in adipogenesis and metabolism, with their corresponding localization on PINK1 promoter region were listed.

Conflicts of Interest

The authors declare no conflict of interest.

REFERENCES

[1] Zimmet P, Alberti KG, Shaw J. Global and societal implications of the diabetes epidemic. Nature 2001;414:782–7.
[2] Camp HS, Ren D, Leff T. Adipogenesis and fat-cell function in obesity and diabetes. Trends Mol Med 2002;8:442–7.
[3] Zhang Y, Zeng X, Jin S. Autophagy in adipose tissue biology. Pharmacol Res 2012;66:505–12.
[4] Kusminski CM, Scherer PE. Mitochondrial dysfunction in white adipose tissue. Trends Endocrinol Metab 2012;23:435–43.
[5] Fruhbeck G, Gomez-Ambrosi J, Muruzabal FJ, Burrell MA. The adipocyte: a model for integration of endocrine and metabolic signaling in energy metabolism regulation. Am J Physiol Endocrinol Metab 2011;80:E827–47.
[6] Detmer SA, Chan DC. Functions and dysfunctions of mitochondrial dynamics. Nat Rev Mol Cell Biol 2007;8:870–9.
[7] Westermann B. Mitochondrial fusion and fission in cell life and death. Nat Rev Mol Cell Biol 2010;11:872–84.
[8] Kitada T, Asakawa S, Hattori N, Matsumine H, Yamamura Y, Minoshima S, et al. Mutations in the parkin gene cause autosomal recessive juvenile parkinsonism. Nature 1998;392:605–8.
[9] Sim CH, Lio DS, Mok SS, Masters CL, Hill AF, Culvenor JG, et al. C-terminal truncation and Parkinson's disease-associated mutations down-regulate the protein serine/threonine kinase activity of PTEN-induced kinase-1. Hum Mol Genet 2006;15:3251–62.

[10] Valente EM, Abou-Sleiman PM, Caputo V, Muqit MM, Harvey K, Gispert S, et al. Hereditary early-onset Parkinson's disease caused by mutations in PINK1. Science 2004;304:1158–60.
[11] Menzies FM, Fleming A, Rubinsztein DC. Compromised autophagy and neurodegenerative diseases. Nat Rev Neurosci 2015;16:345–57.
[12] Civitarese AE, Ukropcova B, Carling S, Hulver M, DeFronzo RA, Mandarino L, et al. Role of adiponectin in human skeletal muscle bioenergetics. Cell Metab 2006;4:75–87.
[13] Franks PW, Scheele C, Loos RJ, Nielsen AR, Finucane FM, Wahlestedt C, et al. Genomic variants at the PINK1 locus are associated with transcript abundance and plasma nonesterified fatty acid concentrations in European whites. FASEB J 2008;22:3135–45.
[14] Scheele C, Nielsen AR, Walden TB, Sewell DA, Fischer CP, Brogan RJ, et al. Altered regulation of PINK1 locus: a link between type 2 diabetes and neurodengeneration? FASEB J 2007;21:3653–65.
[15] Tamguney T, Stokoe D. New insights into PTEN. J Cell Sci 2007;120:4071–9.
[16] Wymann MP, Schneiter R. Lipid signalling in disease. Nat Rev Mol Cell Biol 2008;9:162–76.
[17] Barbeau A, Pourcher E. New data on the genetics of Parkinson's disease. Can J Neurol Sci 1982;9:53–60.
[18] Boyd III AE, Lebovitz HE, Feldman JM. Endocrine function and glucose metabolism in patients with Parkinson's disease and their alternation by L-Dopa. J Clin Endocrinol Metab 1971;33:829–37.
[19] Lipman IJ, Boykin ME, Flora RE. Glucose intolerance in Parkinson's disease. J Chronic Dis 1974;27:573–9.
[20] Sandyk R. The relationship between diabetes mellitus and Parkinson's disease. Int J Neurosci 1993;69:125–30.
[21] Hu G, Jousilahti P, Bidel S, Antikainen R, Tuomilehto J. Type 2 diabetes and risk of Parkinson's disease. Diabetes Care 2007;30:842–7.
[22] Tsao CH, Shiau MY, Chuang PH, Chang YH, Hwang J. Interleukin-4 regulates lipid metabolism by inhibiting adipogenesis and promoting lipolysis. J Lipid Res 2014;55:385–97.
[23] Chang YH, Ho KT, Lu SH, Huang CN, Shiau MY. Regulation of glucose/lipid metabolism and insulin sensitivity by interleukin-4. Int J Obes (Lond) 2012;36:993–8.
[24] Ong SB, Subrayan S, Lim SY, Yellon DM, Davidson SM, Hausenloy DJ. Inhibiting mitochondrial fission protects the heart against ischemia/reperfusion injury. Circulation 2010;121:2012–22.
[25] Rabinowitz JD, White E. Autophagy and metabolism. Science 2010;330:1344–8.
[26] Ravikumar B, Sarkar S, Davies JE, Futter M, Garcia-Arencibia M, Green-Thompson ZW, et al. Regulation of mammalian autophagy in physiology and pathophysiology. Physiol Rev 2010;90:1383–435.
[27] Deas E, Plun-Favreau H, Gandhi S, Desmond H, Kjaer S, Loh SH, et al. PINK1 cleavage at position A103 by the mitochondrial protease PARL. Hum Mol Genet 2011;20:867–79.
[28] Clark IE, Dodson MW, Jiang C, Cao JH, Huh JR, Seol JH, et al. Drosophila pink1 is required for mitochondrial function and interacts genetically with Parkin. Nature 2006;441:1162–6.
[29] Park J, Lee SB, Lee S, Kim Y, Song S, Kim S, et al. Mitochondrial dysfunction in drosophila PINK1 mutants is complemented by parkin. Nature 2006;441:1157–61.
[30] Poole AC, Thomas RE, Andrews LA, McBride HM, Whitworth AJ, Pallanck LJ. The PINK1/Parkin pathway regulates mitochondrial morphology. Proc Natl Acad Sci U S A 2008;105:1638–43.
[31] Lutz A, Exner N, Fett M, Schlehe J, Kloos K, Lämmermann K, et al. Loss of parkin or PINK1 function increases Drp1-dependent mitochondrial fragmentation. J Biol Chem 2009;284:22938–51.
[32] Hauner H, Röhrig K, Spelleken M, Liu LS, Eckel J. Development of insulin-responsive glucose uptake and GLUT4 expression in differentiating human adipocyte precursor cells. Int J Obes Relat Metab Disord 1998;22:448–553.
[33] Hatunic M, Stapleton M, Hand E, DeLong C, Crowley VE, Nolan JJ. The Leu262Val polymorphism of presenilin associated rhomboid like protein (PARL) is associated with earlier onset of type 2 diabetes and increased urinary microalbumin creatinine ratio in an Irish case-control population. Diabetes Res Clin Pract 2009;83:316–9.
[34] Direk K, Lau W, Small KS, Maniatis N, Andrew T. ABCC5 transporter is a novel type 2 diabetes susceptibility gene in European and African American populations. Ann Hum Genet 2014;78:333–44.
[35] Unoki M, Nakamura Y. Growth-suppressive effects of BPOZ and EGR2, two genes involved in the PTEN signaling pathway. Oncogene 2001;20:4457–65.
[36] Civitarese AE, MacLean PS, Carling S, Kerr-Bayles L, McMillan RP, Pierce A, et al. Regulation of skeletal muscle oxidative capacity and insulin signaling by the mitochondrial rhomboid protease PARL. Cell Metab 2010;11:412–26.
[37] Lowell BB, Shulman GI. Mitochondrial dysfunction and type 2 diabetes. Science 2005;307:384–7.
[38] Petersen KF, Dufour S, Befroy D, Garcia R, Shulman GI. Impaired mitochondrial activity in the insulin-resistant offspring of patients with type 2 diabetes. N Engl J Med 2004;350:664–71.
[39] Turner N, Heilbronn LK. Is mitochondrial dysfunction a cause of insulin resistance? Trends Endocrinol Metab 2008;19:324–30.
[40] Jin HS, Kim J, Lee SJ, Kim K, Go MJ, Lee JY, et al. The PARK2 gene is involved in the maintenance of pancreatic β-cell functions related to insulin production and secretion. Mol Cell Endocrinol 2014;382:178–89.
[41] Kelley DE, Goodpaster B, Wing RR, Simoneau JA. Skeletal muscle fatty acid metabolism in association with insulin resistance, obesity, and weight loss. Am J Phys 1999;277:E1130–41.
[42] Goodpaster BH, Thaete FL, Simoneau JA, Kelley DE. Subcutaneous abdominal fat and thigh muscle composition predict insulin sensitivity independently of visceral fat. Diabetes 1997;46:1579–85.
[43] Kelley DE, He J, Menshikova EV, Ritov VB. Dysfunction of mitochondria in human skeletal muscle in type 2 diabetes. Diabetes 2002;51:2944–50.
[44] Kelley DE, Mandarino LJ. Fuel selection in human skeletal muscle in insulin resistance: a reexamination. Diabetes 2000;49:677–83.
[45] Goldman SJ, Zhang Y, Jin S. Autophagic degradation of mitochondria in white adipose tissue differentiation. Antioxid Redox Signal 2011;14:1971–8.
[46] Yang Y, Gehrke S, Haque ME, Imai Y, Kosek J, Yang L, et al. Inactivation of drosophila DJ-1 leads to impairments of oxidative stress response and phosphatidylinositol 3-kinase/Akt signaling. Proc Natl Acad Sci U S A 2005;102:13670–5.
[47] Ries V, Henchcliffe C, Kareva T, Rzhetskaya M, Bland R, During MJ. Oncoprotein Akt/PKB induces trophic effects in murine models of Parkinson's disease. Proc Natl Acad Sci U S A 2006;103:18757–62.
[48] Huang S, Wang Y, Gan X, Fang D, Zhong C, Wu L, et al. Drp1-mediated mitochondrial abnormalities link to synaptic injury in diabetes model. Diabetes 2015;64:1728–42.
[49] Khang R, Park C, Shin JH. Dysregulation of parkin in the substantia nigra of db/db and high-fat diet mice. Neuroscience 2015;294:182–92.
[50] Lin W, Kang UJ. Characterization of PINK1 processing, stability, and subcellular localization. J Neurochem 2008;106:464–74.